

1 Supplementary A

2 Optimal Control Model Details

3 We setup two optimal feedback controllers, each representing one participant, that move a jointly
 4 controlled midpoint. Each optimal controller considered its own states, the position of the jointly
 5 controlled midpoint, and the position and velocity of their partner's hand. As described in the
 6 **Methods** section, the states of the controller representing the left side participant's hand are as
 7 follows.

$$x_t = [p_m^x \ p_m^y \ X_l \ X_r \ p_{target}^x \ p_{target}^y]^T \quad (1)$$

8 where p_m^x and p_m^y are the position coordinates of the jointly controlled midpoint, p_{target}^x and p_{target}^y
 9 are the position coordinates of the target. X_l represents its own states and X_r represents their
 10 partner's (right side participant's hand) states, which are expanded as follows:

$$X_l = [p_{lc}^x \ v_{lc}^x \ p_l^x \ p_l^y \ v_l^x \ v_l^y \ f_l^x \ g_l^x \ f_l^y \ g_l^y] \quad (2)$$

$$X_r = [p_{rc}^x \ v_{rc}^x \ p_r^x \ p_r^y \ v_r^x \ v_r^y] \quad (3)$$

11 where, p_{lc}^x , p_{rc}^x are the lateral cursor positions, v_{lc}^x , v_{rc}^x are the lateral cursor velocities, p_l^x , p_l^y , p_r^x , p_r^y
 12 are the position coordinates of the hands, v_l^x , v_l^y , v_r^x , v_r^y are the velocity states of the hands, and
 13 f_l^x , f_l^y , g_l^x , g_l^y are the states of the second order, low-pass filter. As a reminder, we maintained
 14 separate states for the cursor (p_{lc}^x , v_{lc}^x , p_{rc}^x , v_{rc}^x) and the hand (p_l^x , v_l^x , p_r^x , v_r^x) in the lateral dimension
 15 to accommodate lateral cursor jumps caused by visual perturbations.

16 State Feedback Design

17 To include state feedback delays, we augmented the state vector with previous states (**Eq. 4**).
 18 This allowed the observer to access delayed states, including delayed haptic feedback (Δh) and
 19 delayed visual feedback (Δv) according to:

$$\mathbf{x}_t = \begin{bmatrix} x_t & x_{t-1} & \dots & x_{t-\Delta h} & \dots & x_{t-\Delta v} \end{bmatrix} \quad (4)$$

20 where, t represents a time step with step size 10 ms, $\Delta h = 5$ (50 ms),¹ and $\Delta v = 10$ (100 ms).²

21 Then the observations made by the controller were formulated as

$$y_t = H\mathbf{x}_t + \omega_t \quad (5)$$

22 where, $y_t \in \mathbb{R}^{n_y}$ is the vector of delayed state observations. The covariance of the sensory
 23 noise Ω^ω was a matrix with the corresponding state noise standard deviations along the diagonal.
 24 Sensory noise (i.e., proportional to variance), $\omega_t \in \mathbb{R}^{n_y}$, is modeled using a multidimensional
 25 gaussian random variable with zero mean and covariance Ω^ω . We set the standard deviations for
 26 position ($\sigma = 0.01m$), velocity ($\sigma = 0.1m/s$) and force state ($\sigma = 1N$) noise.³ This noise was scaled
 27 by partner haptic feedback (0.8), self proprioceptive feedback (0.4), and partner and self visual
 28 feedback (0.2) to capture the unique sensory variance associated with each form of feedback.

29 Aligned with experiment conditions, the observation matrix H was designed to selectively
 30 observe the states delayed by haptic and/or visual feedback.

$$H = \begin{bmatrix} 0 & \dots & h_h & \dots & 0 \\ 0 & \dots & 0 & \dots & h_v \end{bmatrix} \quad (6)$$

31 where, for example, the h_h and h_v matrices for the left side controller when observing both visual
 32 and haptic feedback of the partner are as follows:

$$h_h = \begin{bmatrix} 0 & 0 & 0 & 0 & 1 & 0 & 0 & 0 & 0 & 0 & 0 & 0 & 0 & 0 & 0 & 0 & 0 & 0 & 0 & 0 & 0 \\ 0 & 0 & 0 & 0 & 0 & 1 & 0 & 0 & 0 & 0 & 0 & 0 & 0 & 0 & 0 & 0 & 0 & 0 & 0 & 0 & 0 \\ 0 & 0 & 0 & 0 & 0 & 0 & 1 & 0 & 0 & 0 & 0 & 0 & 0 & 0 & 0 & 0 & 0 & 0 & 0 & 0 & 0 \\ 0 & 0 & 0 & 0 & 0 & 0 & 0 & 1 & 0 & 0 & 0 & 0 & 0 & 0 & 0 & 0 & 0 & 0 & 0 & 0 & 0 \\ 0 & 0 & 0 & 0 & 0 & 0 & 0 & 0 & 1 & 0 & 0 & 0 & 0 & 0 & 0 & 0 & 0 & 0 & 0 & 0 & 0 \\ 0 & 0 & 0 & 0 & 0 & 0 & 0 & 0 & 0 & 1 & 0 & 0 & 0 & 0 & 0 & 0 & 0 & 0 & 0 & 0 & 0 \\ 0 & 0 & 0 & 0 & 0 & 0 & 0 & 0 & 0 & 0 & 1 & 0 & 0 & 0 & 0 & 0 & 0 & 0 & 0 & 0 & 0 \\ 0 & 0 & 0 & 0 & 0 & 0 & 0 & 0 & 0 & 0 & 0 & 1 & 0 & 0 & 0 & 0 & 0 & 0 & 0 & 0 & 0 \\ 0 & 0 & 0 & 0 & 0 & 0 & 0 & 0 & 0 & 0 & 0 & 0 & 1 & 0 & 0 & 0 & 0 & 0 & 0 & 0 & 0 \\ 0 & 0 & 0 & 0 & 0 & 0 & 0 & 0 & 0 & 0 & 0 & 0 & 0 & 1 & 0 & 0 & 0 & 0 & 0 & 0 & 0 \\ 0 & 0 & 0 & 0 & 0 & 0 & 0 & 0 & 0 & 0 & 0 & 0 & 0 & 0 & 1 & 0 & 0 & 0 & 0 & 0 & 0 \\ 0 & 0 & 0 & 0 & 0 & 0 & 0 & 0 & 0 & 0 & 0 & 0 & 0 & 0 & 0 & 1 & 0 & 0 & 0 & 0 & 0 \\ 0 & 0 & 0 & 0 & 0 & 0 & 0 & 0 & 0 & 0 & 0 & 0 & 0 & 0 & 0 & 0 & 1 & 0 & 0 & 0 & 0 \\ 0 & 0 & 0 & 0 & 0 & 0 & 0 & 0 & 0 & 0 & 0 & 0 & 0 & 0 & 0 & 0 & 0 & 1 & 0 & 0 & 0 \end{bmatrix} \quad (7)$$

33

$$h_v = \begin{bmatrix} 0 & 0 & 1 & 0 & 0 & 0 & 0 & 0 & 0 & 0 & 0 & 0 & 0 & 0 & 0 & 0 & 0 & 0 & 0 & 0 \\ 0 & 0 & 0 & 1 & 0 & 0 & 0 & 0 & 0 & 0 & 0 & 0 & 0 & 0 & 0 & 0 & 0 & 0 & 0 & 0 \\ 0 & 0 & 0 & 0 & 1 & 0 & 0 & 0 & 0 & 0 & 0 & 0 & 0 & 0 & 0 & 0 & 0 & 0 & 0 & 0 \\ 0 & 0 & 0 & 0 & 0 & 1 & 0 & 0 & 0 & 0 & 0 & 0 & 0 & 0 & 0 & 0 & 0 & 0 & 0 & 0 \\ 0 & 0 & 0 & 0 & 0 & 0 & 1 & 0 & 0 & 0 & 0 & 0 & 0 & 0 & 0 & 0 & 0 & 0 & 0 & 0 \\ 0 & 0 & 0 & 0 & 0 & 0 & 0 & 1 & 0 & 0 & 0 & 0 & 0 & 0 & 0 & 0 & 0 & 0 & 0 & 0 \\ 0 & 0 & 0 & 0 & 0 & 0 & 0 & 0 & 1 & 0 & 0 & 0 & 0 & 0 & 0 & 0 & 0 & 0 & 0 & 0 \\ 0 & 0 & 0 & 0 & 0 & 0 & 0 & 0 & 0 & 1 & 0 & 0 & 0 & 0 & 0 & 0 & 0 & 0 & 0 & 0 \\ 0 & 0 & 0 & 0 & 0 & 0 & 0 & 0 & 0 & 0 & 1 & 0 & 0 & 0 & 0 & 0 & 0 & 0 & 0 & 0 \\ 0 & 0 & 0 & 0 & 0 & 0 & 0 & 0 & 0 & 0 & 0 & 1 & 0 & 0 & 0 & 0 & 0 & 0 & 0 & 0 \\ 0 & 0 & 0 & 0 & 0 & 0 & 0 & 0 & 0 & 0 & 0 & 0 & 1 & 0 & 0 & 0 & 0 & 0 & 0 & 0 \\ 0 & 0 & 0 & 0 & 0 & 0 & 0 & 0 & 0 & 0 & 0 & 0 & 0 & 1 & 0 & 0 & 0 & 0 & 0 & 0 \\ 0 & 0 & 0 & 0 & 0 & 0 & 0 & 0 & 0 & 0 & 0 & 0 & 0 & 0 & 1 & 0 & 0 & 0 & 0 & 0 \\ 0 & 0 & 0 & 0 & 0 & 0 & 0 & 0 & 0 & 0 & 0 & 0 & 0 & 0 & 0 & 1 & 0 & 0 & 0 & 0 \\ 0 & 0 & 0 & 0 & 0 & 0 & 0 & 0 & 0 & 0 & 0 & 0 & 0 & 0 & 0 & 0 & 1 & 0 & 0 & 0 \\ 0 & 0 & 0 & 0 & 0 & 0 & 0 & 0 & 0 & 0 & 0 & 0 & 0 & 0 & 0 & 0 & 0 & 1 & 0 & 0 \end{bmatrix} \quad (8)$$

34 The posterior state estimate \hat{x}_t is obtained online using a filter of the form:

$$\hat{x}_t = x_t^p + K_t(y_t - x_t^p) \quad (9)$$

$$x_t^p = f(\hat{x}_{t-1}, u_{t-1}) \quad (10)$$

35 where, $\hat{x}_{t|t-1}$ is the internal prior prediction of the state given previous state estimate \hat{x}_{t-1} and the
 36 efference copy u_{t-1} . The Kalman filter gains K_t were obtained adaptively by forward recursion
 37 of **Eq. 11**. The covariance of the initial state estimate \hat{x}_1 is Σ_1 .

$$K_t = \Sigma_t H^T (H \Sigma_t H^T + \Omega^\omega)^{-1} \quad (11)$$

$$\Sigma_{t+1} = A_t \Sigma_t A_t^T + \Omega^\epsilon \quad \Sigma_1 = I_{20}$$

38

39 Optimal Control Design

40 For controller design, we setup the total cost at the initial step J_1 in the following quadratic form:

$$J_1 = \frac{1}{2}(x_N + \delta x_N)^T Q_N(x_N + \delta x_N) + \frac{1}{2} \sum_{t=1}^{N-1} (x_t + \delta x_t)^T Q(x_t + \delta x_t) + (u_t + \delta u_t)^T R(u_t + \delta u_t) \quad (12)$$

⁴¹ where, the final state cost matrix Q_N , and the control cost matrix R were designed as follows:

$$P = \begin{bmatrix} -w_p & 0 & 0 & 0 & 0 & 0 & 0 & 0 & 0 & 0 & 0 & 0 & 0 & 0 & 0 & 0 & w_p & 0 \\ 0 & -w_p & 0 & 0 & 0 & 0 & 0 & 0 & 0 & 0 & 0 & 0 & 0 & 0 & 0 & 0 & 0 & w_p \\ 0 & 0 & 0 & 0 & 0 & 0 & 0 & 0 & 0 & 0 & 0 & 0 & 0 & 0 & 0 & 0 & 0 & 0 \\ 0 & 0 & 0 & w_v & 0 & 0 & 0 & 0 & 0 & 0 & 0 & 0 & 0 & 0 & 0 & 0 & 0 & 0 \\ 0 & 0 & 0 & 0 & 0 & 0 & 0 & 0 & 0 & 0 & 0 & 0 & 0 & 0 & 0 & 0 & 0 & 0 \\ 0 & 0 & 0 & 0 & 0 & 0 & 0 & 0 & 0 & 0 & 0 & 0 & 0 & 0 & 0 & 0 & 0 & 0 \\ 0 & 0 & 0 & 0 & 0 & 0 & 0 & 0 & 0 & 0 & 0 & 0 & 0 & 0 & 0 & 0 & 0 & 0 \\ 0 & 0 & 0 & 0 & 0 & 0 & 0 & 0 & 0 & 0 & 0 & 0 & 0 & 0 & 0 & 0 & 0 & 0 \\ 0 & 0 & 0 & 0 & 0 & 0 & 0 & 0 & 0 & 0 & 0 & 0 & 0 & 0 & 0 & 0 & 0 & 0 \\ 0 & 0 & 0 & 0 & 0 & 0 & 0 & 0 & 0 & 0 & 0 & 0 & 0 & 0 & 0 & 0 & 0 & 0 \\ 0 & 0 & 0 & 0 & 0 & 0 & 0 & 0 & 0 & 0 & 0 & 0 & 0 & 0 & 0 & 0 & 0 & 0 \\ 0 & 0 & 0 & 0 & 0 & 0 & 0 & 0 & 0 & 0 & 0 & 0 & 0 & 0 & 0 & 0 & 0 & 0 \\ 0 & 0 & 0 & 0 & 0 & 0 & 0 & 0 & 0 & 0 & 0 & 0 & 0 & 0 & 0 & 0 & 0 & 0 \\ 0 & 0 & 0 & 0 & 0 & 0 & 0 & 0 & 0 & 0 & 0 & 0 & 0 & 0 & 0 & 0 & 0 & 0 \\ 0 & 0 & 0 & 0 & 0 & 0 & 0 & 0 & 0 & 0 & 0 & 0 & 0 & 0 & 0 & 0 & 0 & 0 \\ 0 & 0 & 0 & 0 & 0 & 0 & 0 & 0 & 0 & 0 & 0 & 0 & 0 & 0 & 0 & 0 & 0 & 0 \\ 0 & 0 & 0 & 0 & 0 & 0 & 0 & 0 & 0 & 0 & 0 & 0 & 0 & 0 & 0 & 0 & 0 & 0 \\ 0 & 0 & 0 & 0 & 0 & 0 & 0 & 0 & 0 & 0 & 0 & 0 & 0 & 0 & 0 & 0 & 0 & 0 \end{bmatrix} \quad (13)$$

$$Q_N = \frac{1}{2} P^T P, \quad Q = 0$$

⁴²

$$R = r \begin{bmatrix} 1 & 0 \\ 0 & 1 \end{bmatrix} \quad (14)$$

⁴³ where, the state cost scaling terms are $w_p = 1$, $w_v = 0.2$, and $w_f = 0.01$, and the control cost
⁴⁴ scaling term is $r = 0.003$. The state-feedback controller for the above control problem is as
⁴⁵ follows:

$$\delta u_t = -L_t \delta \hat{x}_t - L_t^v v_{t+1} - L_t^u u_t \quad (15)$$

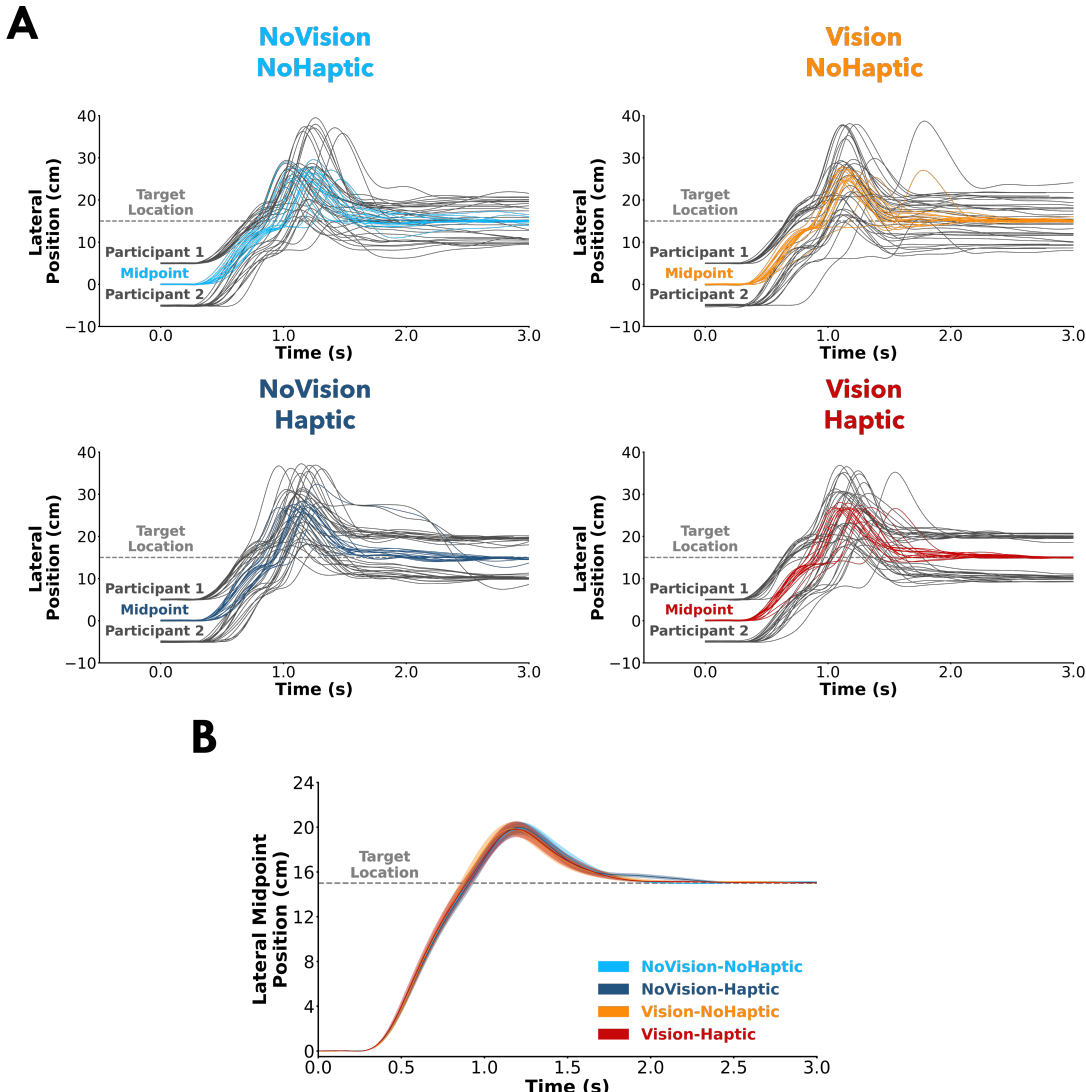
⁴⁶ Where, $\delta \hat{x}_t = \hat{x}_t - x_t$ is an unbiased estimate of the state deviation. The state estimate \hat{x}_t is
⁴⁷ updated recursively (**Eq. 9-11**) using an Extended Kalman Filter. The feedback gains L_t , L_t^v , and
⁴⁸ L_t^u were obtained by backward recursion:

$$\begin{aligned} L_t &= (R + B_t^T S_{t+1} B_t)^{-1} B_t^T S_{t+1} A_t \\ L_t^v &= (R + B_t^T S_{t+1} B_t)^{-1} B_t \\ L_t^u &= (R + B_t^T S_{t+1} B_t)^{-1} R \\ S_t &= Q_t + A_t^T S_{t+1} (A_t - B_t L_t) & S_N^x &= Q_N \\ v_t &= (A_t - B_t L_t)^T v_{t+1} - L_t^T R u_t^* + Q_t x_t^* & v_N &= Q_N x_N \end{aligned} \quad (16)$$

⁴⁹ where, A_t , B_t form the linearized system obtained around the nominal trajectory (u_t^*, x_t^*) as de-
⁵⁰ scribed in the **Methods** section.

51 **Supplementary B**52 **Experiment 1 Movement Trajectories During Mechanical Perturbation Trials**

53



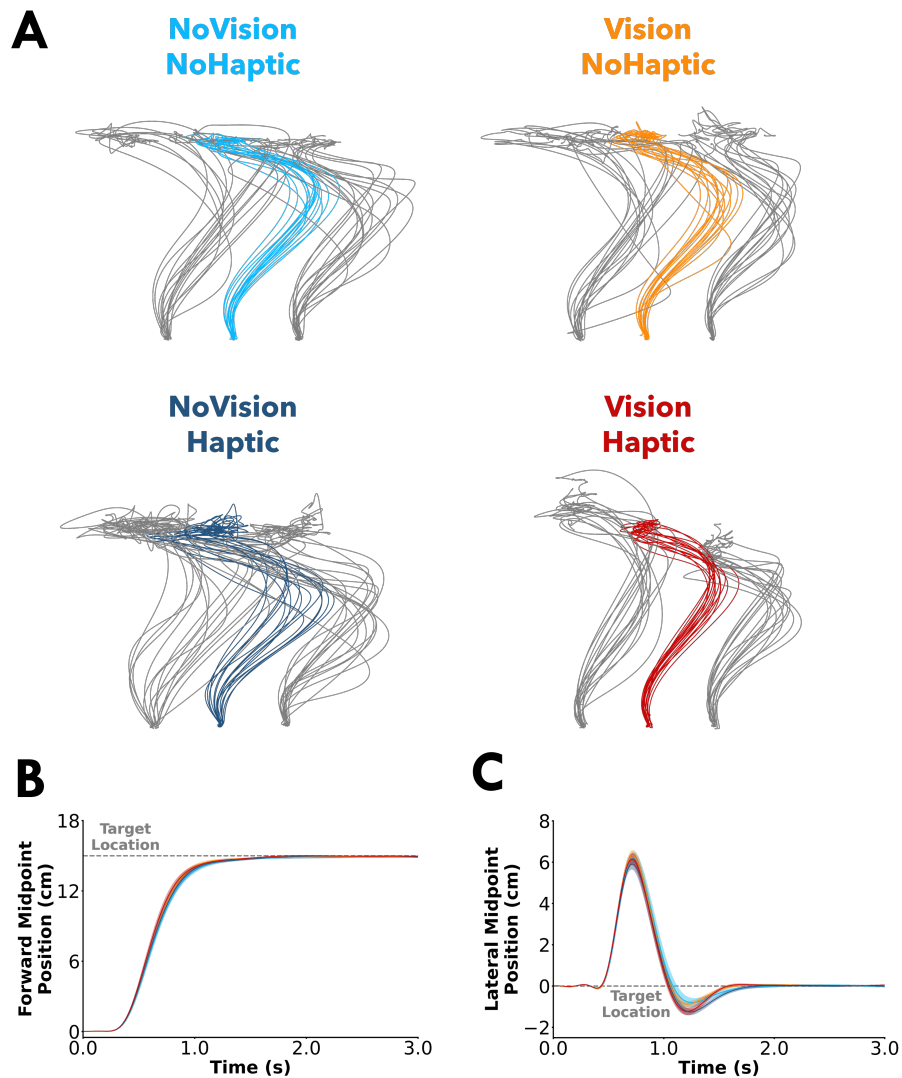
55

56 **Figure S1: Experiment 1 participant hand and midpoint movement behaviour for mechanical perturbation**
 57 **trials. A)** Lateral hand (cursor) position and lateral midpoint position (y-axis) over time (x-axis) from an exemplar
 58 human pair. Participant 1 and 2 hand trajectories are grey and the midpoint trajectories are coloured according to
 59 the respective condition. **B)** Mean lateral midpoint position (y-axis) over trial time (x-axis) for each condition. Error
 60 ribbons represent ± 1 standard error between human pairs.

61 Individual participant hand trajectories and jointly controlled midpoint trajectories from an
62 exemplar human pair are shown for the mechanical perturbation trials of each feedback condition
63 (**Fig. S1A**). After receiving mechanical perturbations, the human pair worked in unison to stabilize
64 the jointly controlled midpoint at the target. At the group level, across all human pairs, we show
65 the average lateral midpoint position (**Fig. S1B**). Participants displayed a similar lateral midpoint
66 position across conditions.

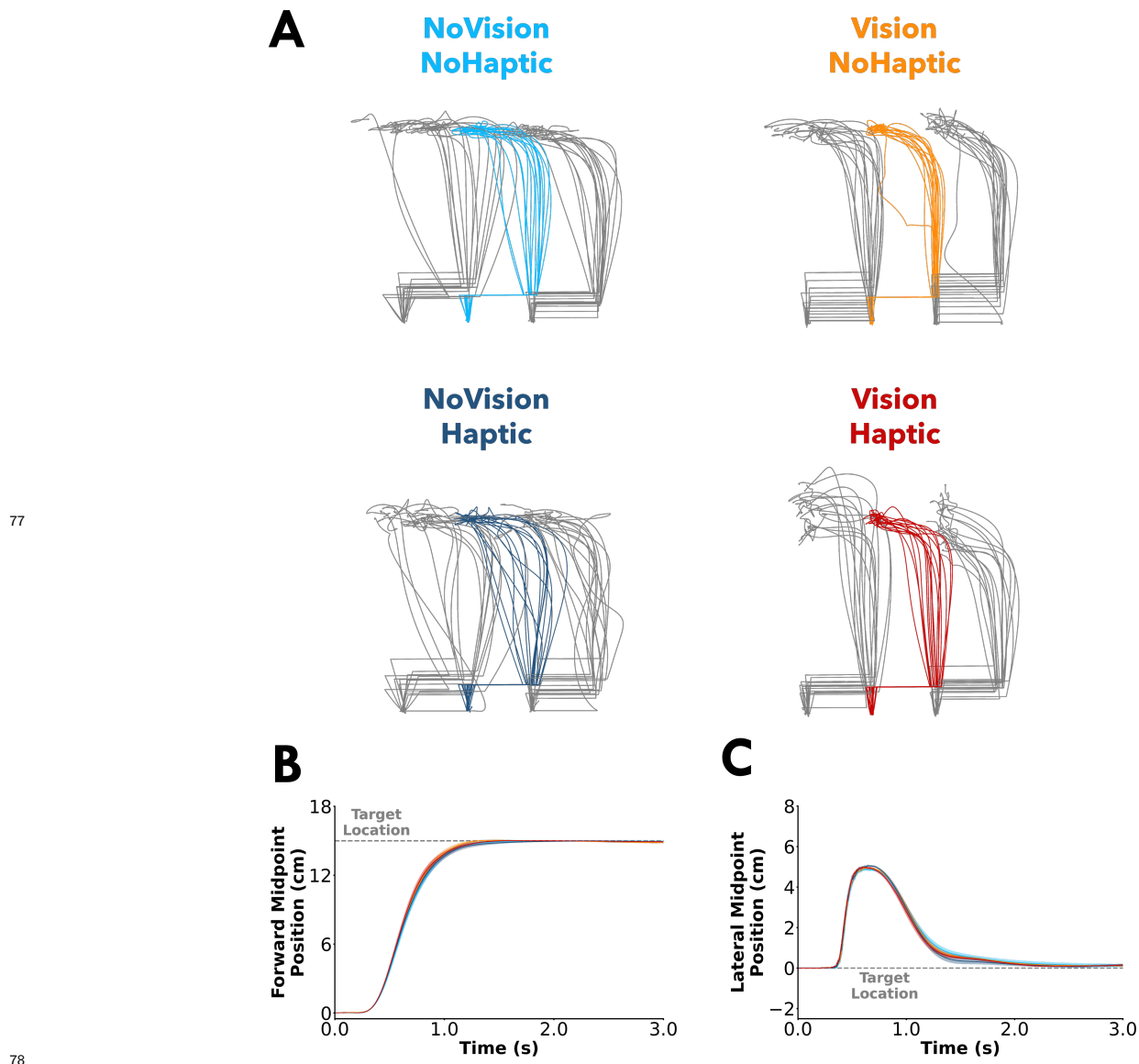
67 **Supplementary C**68 **Experiment 2 Movement Trajectories During Mechanical Perturbation Trials**

69



70

Figure S2: Experiment 2 participant hand and midpoint movement behaviour for mechanical perturbation trials. **A)** Lateral hand (cursor) position and lateral midpoint position (y-axis) over time (x-axis) from an exemplar human pair. Participant 1 and 2 cursor trajectories are grey and the midpoint trajectories are coloured according to the respective condition. **B)** Mean forward midpoint position (y-axis) and **C)** mean lateral midpoint position (y-axis) over trial time (x-axis).



79 **Figure S3: Experiment 2 participant hand and midpoint movement behaviour for visual perturbation trials.**
80 **A)** Lateral hand (cursor) position and lateral midpoint position (y-axis) over time (x-axis) from an exemplar human pair.
81 Participant 1 and 2 cursor trajectories are grey and the midpoint trajectories are coloured according to the respective
82 condition. Note that the cursor trajectory (shown) of each participant would be different from their hand trajectory
83 for the visual perturbation trials specifically after the cursor was jumped laterally by 5 cm. **B)** Mean forward midpoint
84 position (y-axis) and **C)** mean lateral midpoint position (y-axis) over trial time (x-axis).

Individual participant hand trajectories and jointly controlled midpoint trajectories from an exemplar human pair are shown for mechanical perturbation trials (**Fig. S2A**) and visual perturbation trials (**Fig. S3A**) of each feedback condition. After receiving mechanical perturbations or visual perturbations, the human pair worked in unison to stabilize the jointly controlled midpoint at the target. At the group level, across all human pairs, we show the average forward midpoint position (**Fig. S2B**) and average lateral midpoint position (**Fig. S2C**) for mechanical perturbation trials. At the group level, across all human pairs, we show the average forward midpoint position (**Fig. S3B**) and average lateral midpoint position (**Fig. S3C**) for visual perturbation trials.

References

1. Scott, S. H. (2012). The computational and neural basis of voluntary motor control and planning. en. *Trends in Cognitive Sciences*, 16 (11), 541–549.
2. Izawa, J., & Shadmehr, R. (2008). On-Line Processing of Uncertain Information in Visuomotor Control. en. *Journal of Neuroscience*, 28 (44), 11360–11368.
3. Todorov, E. (2005). Stochastic Optimal Control and Estimation Methods Adapted to the Noise Characteristics of the Sensorimotor System. *Neural Computation*, 17 (5), 1084–1108.